Molecular Orbital Study of Crystalline Acetic Acid. 2. Aggregates in One, Two, and Three Dimensions

László Turi† and J. J. Dannenberg*

Contribution from the Department of Chemistry, Hunter College and The Graduate School, City University of New York, 695 Park Avenue, New York, New York 10021

Received November 16, 1993. Revised Manuscript Received April 4, 1994®

Abstract: Ab initio and semiempirical molecular orbital calculations on aggregates containing up to 36 molecules of acetic acid are presented. Aggregation is considered in three directions: (a) H-bonding interactions involving O—H···O and C—H···O interactions to form "chains"; (b) "stacking" of the chains through weak C—H···O interactions; and (c) assembly of the "stacks" via other C—H···O H-bonding interactions to form "microcrystals". The results provide the first evidence of cooperativity for interactions between different directions as well as within each of the three directions. These cooperative effects are manifest both in the energies of stabilization and in the inter- and intramolecular geometric parameters. An analysis of the interactions between chains (to form stacks) and between stacks (to form microcrystals) shows that pairwise interactions (between either chains or stacks) significantly underestimate the respective interaction energies. The calculations agree reasonably well with the experimental crystal structure but only after all three directions are considered. The results are discussed in terms of the intermolecular forces that operate in processes of molecular recognition and self-assembly such as crystal formation. It is suggested that nonadditive cooperative effects can be extremely important to successful modeling of aggregation and molecular recognition.

Understanding the intermolecular interactions that contribute to molecular recognition is one of the most important chemical problems of our time. While the biochemical aspects of molecular recognition come most readily to mind, the nucleation and crystallization of molecules (as opposed to ions) provide other common examples of this phenomenon. The study of the formation of the molecular aggregates that lead to crystallization provides a useful and convenient means to evaluate the importance of the relevant intermolecular forces. As the crystal units (both molecules and unit cells) are periodic, one can conveniently study large aggregates and even entire crystals. In this manner, one can evaluate the importance of cooperative interactions, as well as simple two-body intermolecular interactions.

Acetic acid provides an ideal subject for study for two reasons: (a) it is sufficiently small so that large aggregates can be studied and (b) the geometry of its dimer is significantly different from its crystal structure. Jones and Templeton[1] reported first the crystal structure of acetic acid in 1958. This structure was reviewed and refined accurately by Nahringbauer.[2] The crystal structures of carboxylic acids have been extensively discussed by Leiserowitz.[3] Unlike most carboxylic acids (for example, propionic acid[4] or fluoroacetic acid[5]), which crystallize as cyclic H-bonding carboxylic acid dimers, acetic acid crystals contain infinite chains of O—H···O H-bonding monomers. They also have important contributions from C—H···O H-bonds. The crystals can be understood by decomposing the structure into interactions in each of three separate directions. In the first direction, the structure is characterized by an infinite chain of H-bonding interactions with one O—H···O and one C—H···O interaction between each pair of molecules (see Figure 1). The second direction involves stacking of these chains (see Figure 2). The third direction is characterized by C—H···O H-bonding interactions between the stacks, with each stack roughly perpendicular to its neighbors (see Figure 3). Despite the fact that, in 1970, Nahringbauer suggested the possible existence of other polymorphs,[2] no other crystal structures of acetic acid have appeared in the literature.

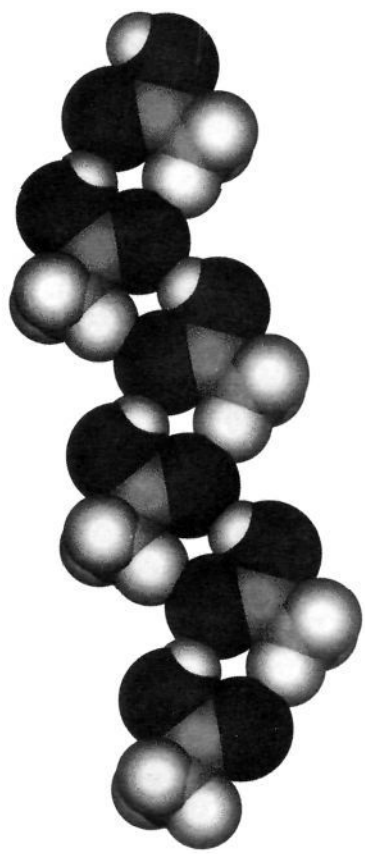

Figure 1. Chain of acetic acid molecules.

In a previous paper on monomers and dimers of acetic acid,[6] we have shown (i) that molecular orbital calculations indicate that the cyclic carboxylic H-bonding dimer **I** has more than twice

† Present address: Department of Physical Chemistry, Eötvös University, Budapest, Hungary.

® Abstract published in *Advance ACS Abstracts,* August 1, 1994.

(1) Jones, R. E.; Templeton, D. H. *Acta Crystallogr.* **1958**, *11*, 484.

(2) Nahringbauer, I. *Acta Chem. Scand.* **1970**, *24*, 453.

(3) Leiserowitz, L. *Acta Crystallogr.* **1976**, *B32*, 775.

(4) Strieter, F. J.; Templeton, D. H.; Scheuerman, R. F.; Sass, R. L. *Acta Crystallogr.* **1962**, *15*, 1233.

(5) Kanters, J. A.; Kroon, J. *Acta Crystallogr.* **1972**, *B8*, 1946.

(6) Turi, L.; Dannenberg, J. J. *J. Phys. Chem.* **1993**, *97*, 12197.

0002-7863/94/1516-8714$04.50/0

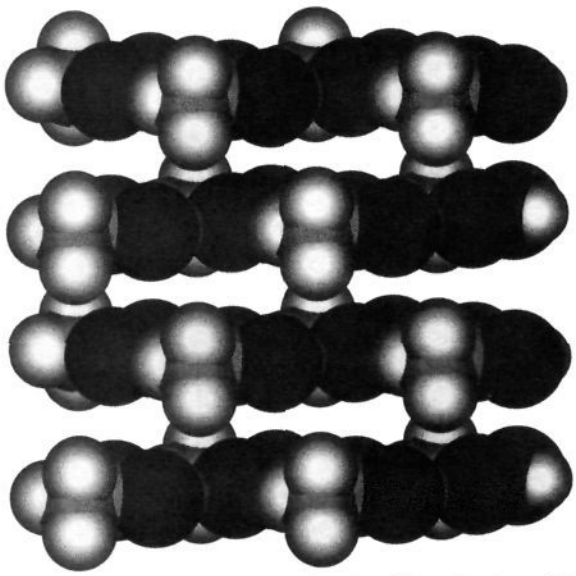

Figure 2. Stack of acetic acid molecules viewed from the edges of the chains.

the stability of a single H-bond and (ii) that the additional C—H···O interaction formed in a dimer (**II**) resembling two adjacent molecules in the first direction defined above is insufficient to overcome the lost cooperativity of the two O—H···O interactions in the "normal" dimer. Thus, the crystal structure must depend upon cooperative interaction between several acetic acid molecules.

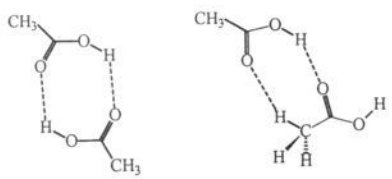

I II

Derissen and Smit[7] have attempted to rationalize the unusual crystal structure using atom–atom potential calculations. Theoretical studies of this type (generally based upon two-body interactions) cannot adequately treat the cooperativity of intermolecular interactions, as documented both by MO calculations[8] and experimental results[9] for H-bonds. We have previously demonstrated[10] the importance of H-bond cooperativity in the crystal structure of 1,3-cyclohexanedione.

In this paper, we report molecular orbital calculations on various acetic acid aggregates in one, two, and three dimensions, containing up to 36 individual molecules.

Methods

Both semiempirical (AM1,[11] PM3,[12] and SAM1[13]) approximations to molecular orbital theory and various levels of ab initio calculations have been used for these studies. The applicability of the AM1 method to H-bonding studies has been reviewed elsewhere.[14] We have previously used it with success in several hydrogen-bonding studies,[15] including modeling of the H-bonding between molecules of various nitroanilines in the crystalline state.[16] Ab initio studies of H-bonding systems are very sensitive to basis set and correction for electron correlation, as exemplified in previous studies of the water dimer,[17,18] hydroxamic acids,[19] and aggregation of 1,3-diones.[10] Calculations of sufficient accuracy on the larger molecular complexes to be considered here are not practical using such costly methods.

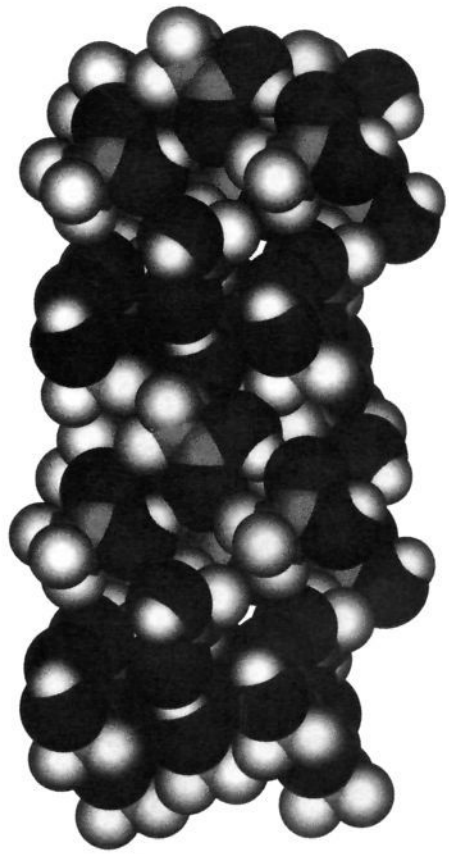

Figure 3. Microcrystal of acetic acid consisting of four stacks of three chains, each containing three molecules (4 × 3 × 3). Note the C—H···O interactions between the stacks.

The geometries of the aggregates were optimized completely with the constraints that the geometry of all molecules in each aggregate be the same and that the heavy atoms in each monomer be in a common plane, with the hydrogen of the hydroxyl group and a hydrogen of the methyl group eclipsed with the carbonyl oxygen. The other two hydrogen atoms have been located symmetrically above and under this plane. In addition, the appropriate translation vectors characteristic of the crystal structure were kept parallel to each other. These constraints are similar to those used by us in previous work. In certain cases, these constraints were removed to test their appropriateness. These constraints allowed us to (a) reduce the complexity of the calculations together with the necessary resources and (b) simplify the analysis of the calculated structure by producing structural parameters that are constant within the system.

The calculations were performed using AMPAC 2.1[20] (AM1),

(7) Derissen, J. L.; Smit, P. H. *Acta Crystallogr.* **1977**, *A33*, 230.
(8) (a) Hodoscek, M.; Kocjan, D.; Hadzi, D. *J. Mol. Struct. (THEOCHEM)* **1988**, *42*, 115. (b) Koehler, J. E. H.; Saenger, W.; Lesyng, B. *J. Comput. Chem.* **1987**, *8*, 1090. Remko, M. *Z. Phys. Chem. (Munich)* **1983**, *138*, 223. Del Bene, J. E. *J. Chem. Phys.* **1980**, *72*, 3423. Tse, Y. C.; Newton, M. D. *J. Am. Chem. Soc.* **1977**, *99*, 611.
(9) (a) Steiner, T.; Mason, S. A.; Saenger, W. *J. Am. Chem. Soc.* **1990**, *112*, 6184. (b) Kleeberg, H.; Luck, W. A. P. *Z. Phys. Chem. (Leipzig)* **1989**, *270*, 613.
(10) Turi, L.; Dannenberg, J. J. *J. Phys. Chem.* **1992**, *96*, 5819.
(11) Dewar, M. J. S.; Zoebisch, E. G.; Healy, E. F.; Stewart, J. J. P. *J. Am. Chem. Soc.* **1985**, *107*, 3902.
(12) Stewart, J. J. P. *J. Comput. Chem.* **1989**, *10*, 209.
(13) Dewar, M. J. S.; Jie, C.; Yu, J. *Tetrahedron* **1993**, *49*, 5003.
(14) Dannenberg, J. J.; Evleth, E. M. *Int. J. Quantum Chem.* **1992**, *44*, 869.
(15) (a) Dannenberg, J. J.; Vinson, L. K. *J. Phys. Chem.* **1988**, *92*, 5635. (b) Galera, S.; Lluch, J. M.; Oliva, A.; Bertrán, J. *J. Mol. Struct. (THEOCHEM)* **1988**, *40*, 101.
(16) Vinson, L. K.; Dannenberg, J. J. *J. Am. Chem. Soc.* **1989**, *111*, 2777.
(17) Dannenberg, J. J. *J. Phys. Chem.* **1988**, *92*, 6869. Dannenberg, J. J.; Mezei, M. *J. Phys. Chem.* **1991**, *95*, 6396.
(18) Smith, B. J.; Swanton, D. J.; Pople, J. A.; Schaefer, H. F., III; Radom, L. *J. Chem. Phys.* **1990**, *92*, 1240.
(19) (a) Turi, L.; Dannenberg, J. J.; Rama, J.; Ventura, O. N. *J. Phys. Chem.* **1992**, *96*, 3709. (b) Ventura, O. N.; Rama, J. B.; Turi, L.; Dannenberg, J. J. *J. Am. Chem. Soc.* **1993**, *115*, 5754.
(20) Graciously furnished by Eamonn Healy and M. J. S. Dewar.

Table 1. Incremental Hydrogen-Bonding Energies (and Enthalpies in AM1, PM3, and SAM1) of Different Acetic Acid Aggregates at Different Levels of Theory without Corrections[a]

	method							
aggregate	AM1	SAM1	PM3	HF/6-31G	HF/6-31G(d)	HF/6-31G(d,p)	MP2/6-31G	MP2/6-31G(d)[b]
dimer I	-6.37	-8.05	-8.86	-19.51	-15.54	-15.50	-18.75	-18.82
dimer II	-4.79	-4.70	-4.87	-11.28	-8.57	-8.59	-10.99	-10.76
	(-4.85)	(-5.04)	(-5.44)	(-11.49)	(-8.75)	(-8.79)	(-11.18)	
trimer II	-4.73	-5.10	-5.40	-11.70	-8.89	-8.90	-11.64	-11.37
	(-4.77)	(-5.20)	(-5.09)	(-11.88)	(-9.02)	(-9.02)		
tetramer II	-4.79	-5.19	-5.51	-11.99	-9.10	-9.11		
	(-4.80)	(-5.26)	(-5.55)	(-12.14)	(-9.18)	(-9.20)		
pentamer II	-4.77	-5.21	-5.54	-12.11	-9.16			
	(-4.78)	(-5.24)	(-5.57)					
hexamer II	-4.79	-5.22	-5.57	-12.17				
	(-4.79)	(-5.25)	(-5.59)					
infinite chains	-4.77	-5.23	-5.57	-12.24	-9.21	-9.55		
	(-4.78)	(-5.26)	(-5.73)	(-12.66)	(-9.41)	(-9.85)		

[a] Values in parentheses correspond to completely optimized structures. Energies in kcal/mol. [b] Frozen core calculations.

AMPAC 4.5[21] (PM3 and SAM1), GAUSSIAN90/GAUSSIAN92[22] (ab initio), and PCMODEL[23] (generation of input and graphics) on IBM RS/6000 RISC computers. The ab initio calculations were performed at both the Hartree–Fock (HF) and the second-order Møller–Plesset (MP2) levels using the 6-31G, 6-31G(d), and 6-31G(d,p) (HF only) basis sets.

All species were completely optimized in all internal coordinates (with the constraints cited above) at *each level of calculation*. Vibrational frequencies were individually calculated at *each level of calculation* to verify the optimizations as well as to provide zero-point vibrational energy corrections (ZPVE) and enthalpies[24] at 298 K for those cases where unconstrained complete optimizations were performed. Vibrational analysis on the constrained structures has little meaning, as they are not true minima on the potential surfaces. The counterpoise (CP) correction for the basis set superposition error (BSSE) for each monomer was calculated as the difference between the energy of the monomer on the complexed geometry with the basis set of the whole complex and that of the same monomer without ghost orbitals.[25,26]

The pairwise interactions between chains were obtained by performing MO calculations on the individual pairs of chains in the orientations and optimized geometries of the larger aggregate and then subtracting the energies of the individual optimized chains. These pairwise interactions consist of the interaction between the chains in the (distorted) geometry they take in the aggregate plus the distortion energy of each chain. The nonadditive part of the interactions is the stabilization of the supermolecule minus the sum of the pairwise interactions. This is often corrected for the different quantity of distortions in each. For the special case where each unit is constrained to the same geometry (thus, the distortion energies are the same for each), it can be shown that this correction is $(n^2 - 2n)$ times the distortion energy.[27]

Results and Discussion

Aggregation in the First Direction: H-Bonding Chains. Figure 1 illustrates the interactions in the first direction, while Figure 4 defines the unit cell parameters. Tables 1 and 2 collect the interaction energies, while Table 3 collects the geometrical data for aggregation in the first direction. The uncorrected energies of Table 1 show that each additional molecule of acetic acid interacts more strongly than the previous one. This is evident for all ab initio methods. The semiempirical methods show much less cooperativity, AM1 almost none. As there are two acetic acid molecules per repeating unit in this direction, the interaction energies do not change monotonically. Eventually, one expects the incremental stabilization to asymptotically approach the value expected for an infinite chain. This value is estimated by fitting

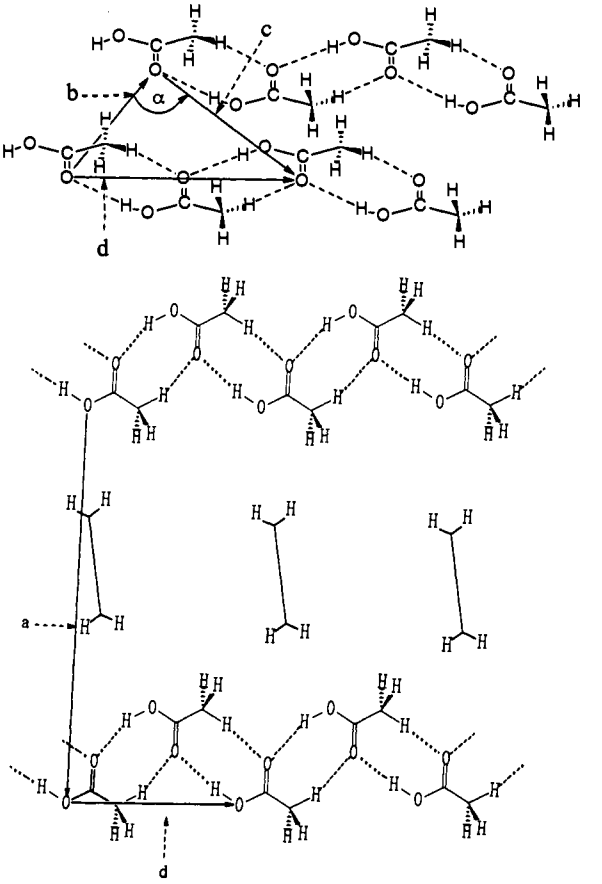

Figure 4. Two different projections of the unit cell of acetic acid illustrating the cell parameters **a**, **b**, **c**, **d**, and α.

an exponential function (eq 1, where a and b are fitted parameters

$$E_n = E_1 - a(1 - e^{-b(n-1)}) \quad (1)$$

for each MO method, n is the number of H-bonds, and E_n is the last H-bonding energy) to the calculated data, as in our previous study of 1,3-diones.[10] We tested the validity of the geometrical constraint of keeping each acetic acid molecule in the same geometry by performining complete optimizations in several cases (indicated in parentheses in Table 1). Clearly, the constraint has only a small effect upon the interaction energies which tends to diminish as the aggregate continues to grow. For example, the difference in the incremental interaction energy at the HF/6-31G(d,p) level decreases from 0.20 to 0.09 kcal/mol upon going from dimer to tetramer.

(21) SemiChem, Inc., Shawnee, KS.
(22) Gaussian, Inc., Pittsburgh, PA.
(23) Serena Software, Bloomington, IN.
(24) Curtiss, L. A. *J. Chem. Phys.* **1977**, *67*, 1144.
(25) Meunier, A.; Levy, B.; Berthier, G. *Theor. Chim. Acta* **1973**, *29*, 49. Boys, S. F.; Bernardi, F. *Mol. Phys.* **1970**, *19*, 553.
(26) Mayer, I.; Surjan, P. R. *Chem. Phys. Lett.* **1992**, *191*, 497. Turi, L.; Dannenberg, J. J. *J. Phys. Chem.* **1993**, *97*, 2488.
(27) A discussion of the problems involved in comparing pairwise and supermolecule calculations will be published elsewhere.

Table 2. Incremental Hydrogen-Bonding Energies and Enthalpies of Different Acetic Acid Aggregates at Different Levels of Theory with CP, ZPVE, and CP + ZPVE Corrections

	method[a]																
	I				II				III				IV				V
aggregate	ΔE_{CP}	ΔE_{ZPE}	ΔE_{CP+ZPE}	ΔH_{298K}	ΔE_{CP}	ΔE_{ZPE}	ΔE_{CP+ZPE}	ΔH_{298K}	ΔE_{CP}	ΔE_{ZPE}	ΔE_{CP+ZPE}	ΔH_{298K}	ΔE_{CP}	ΔE_{ZPE}	ΔE_{CP+ZPE}	ΔH_{298K}	ΔE_{CP}
dimer I	−16.7	−17.8	−15.0	−15.0	−13.1	−13.9	−11.5	−11.3	−13.2	−14.0	−11.7	−11.6	−13.2	−16.8	−11.3	−11.2	−13.5
dimer II	−9.4	−10.0	−8.2	−7.8	−7.0	−7.5	−5.8	−5.4	−7.1	−7.5	−6.0	−5.5	−7.2	−9.6	−5.8	−5.5	−7.2
	(−9.6)	(−10.2)	(−8.4)	(−8.0)	(−7.1)	(−7.6)	(−6.0)	(−5.6)	(−7.2)	(−7.7)	(−6.1)	(−5.7)	(−7.4)	(−9.8)	(−5.9)	(−5.6)	
trimer II	−9.8	−10.6	−8.7	−8.8	−7.2	−7.9	−6.2	−6.3	−7.3				−7.8				−7.7
	(−10.0)	(−10.8)	(−8.9)	(−8.5)	(−7.3)	(−8.0)	(−6.3)	(−5.8)	(−7.4)	(−8.0)	(−6.4)	(−5.9)					
tetramer II	−10.1	−10.9	−9.0	−8.6	−7.4	−8.1	−6.4	−6.5	−7.5								
	(−10.2)	(−11.1)	(−9.2)	(−8.7)	(−7.5)	(−8.2)	(−6.5)	(−6.0)	(−7.6)	(−8.2)	(−6.6)	(−6.1)					
pentamer II	−10.2				−7.5												
hexamer II	−10.3																
infinite chains	−10.3	−11.2	−9.5	−8.8	−7.7	−8.3	−6.6	−6.6	−7.9								
	(−10.4)	(−11.4)	(−9.7)	(−8.8)	(−7.7)	(−8.4)	(−6.9)	(−6.4)	(−8.3)	(−8.4)	(−6.9)	(−7.0)					

[a] Methods: I, HF/6-31G; II, HF/6-31G(d); III, HF/6-31G(d,p); IV, MP2/6-31G (full); V, MP2/6-31G(d) (frozen core). Energies in kcal/mol. Values in parentheses correspond to completely optimized structures.

Table 3. Selected Geometrical Parameters Characteristic of H-Bonding Interactions in One-Dimensional Chains at Different Levels of Theory[a]

	geometrical parameters										
aggregate	C=O	C—O	O···O	O···H(O)	O···C	O···H(C)	α(C=O···H)[c]	α(O—H···O)[c]	β(C=O···H)[c]	β(C—H···O)[c]	translation
						AM1					
dimer	1.237	1.360	3.075	2.104	3.327	2.245	128.2	175.1	139.4	162.3	
trimer	1.238	1.359	3.063	2.093	3.340	2.252	127.0	173.2	137.5	163.5	7.224
tetramer	1.239	1.358	3.059	2.089	3.344	2.254	126.8	172.8	137.1	163.8	7.239
pentamer	1.239	1.357	3.058	2.088	3.346	2.256	126.5	172.4	136.7	164.0	7.255
hexamer	1.239	1.357	3.056	2.086	3.347	2.257	126.4	172.2	136.5	164.1	7.262
						PM3					
dimer	1.223	1.347	2.729	1.792	3.519	2.505	131.1	164.6	133.7	153.0	
trimer	1.225	1.344	2.722	1.784	3.533	2.519	131.1	164.3	133.1	153.0	7.043
tetramer	1.226	1.342	2.720	1.780	3.538	2.523	131.1	164.2	132.8	153.1	7.054
pentamer	1.226	1.341	2.718	1.778	3.541	2.525	131.0	164.1	132.6	153.2	7.061
hexamer	1.227	1.340	2.717	1.777	3.543	2.527	131.0	164.0	132.4	153.3	7.067
						SAM1					
dimer	1.255	1.379	2.740	1.770	2.987	1.906	125.4	171.2	134.9	166.4	
trimer	1.257	1.376	2.729	1.757	2.998	1.915	124.8	170.1	133.8	167.0	6.856
tetramer	1.259	1.374	2.725	1.752	3.001	1.916	124.6	169.8	133.4	167.2	6.866
pentamer	1.259	1.374	2.722	1.749	3.002	1.916	124.5	169.6	133.2	167.3	6.871
hexamer	1.260	1.373	2.721	1.747	3.003	1.916	124.5	169.5	133.1	167.4	6.874
						HF/6-31G					
dimer	1.219	1.341	2.768	1.808	3.407	2.383	138.8	179.2	131.4	158.3	
trimer	1.222	1.336	2.738	1.774	3.489	2.468	138.9	178.4	129.0	157.8	7.003
tetramer	1.224	1.332	2.723	1.757	3.516	2.497	139.3	177.9	128.3	157.4	7.018
pentamer	1.225	1.330	2.713	1.746	3.534	2.517	139.4	177.5	127.7	157.2	7.029
hexamer	1.226	1.329	2.706	1.738	3.546	2.529	139.6	177.2	127.4	157.1	7.035
						HF/6-31G(d)					
dimer	1.194	1.321	2.868	1.918	3.486	2.455	137.7	171.8	130.2	159.5	
trimer	1.196	1.318	2.841	1.891	3.542	2.515	135.4	170.4	128.7	158.8	7.141
tetramer	1.198	1.315	2.829	1.879	3.560	2.534	135.4	169.9	128.0	158.6	7.159
pentamer	1.198	1.314	2.821	1.870	3.517	2.546	135.7	169.9	127.7	158.4	7.159
						HF/6-31G(d,p)					
dimer	1.194	1.320	2.862	1.916	3.470	2.437	134.9	172.1	130.2	159.8	
trimer	1.197	1.316	2.834	1.888	3.524	2.494	135.0	170.5	128.5	159.3	7.139
tetramer	1.198	1.314	2.821	1.874	3.539	2.510	135.2	170.3	127.9	159.1	7.146
						MP2/6-31G					
dimer	1.255	1.387	2.840	1.853	3.395	2.334	133.5	174.8	129.7	163.2	
trimer	1.258	1.380	2.806	1.817	3.438	2.379	133.7	173.4	128.3	162.7	7.177
						MP2/6-31G(d)[b]					
dimer	1.225	1.350	2.838	1.867	3.367	2.310	130.5	168.0	129.2	163.2	
trimer	1.228	1.344	2.808	1.836	3.396	2.341	130.9	167.3	128.3	162.7	7.131
exptl[2]	1.206	1.321	2.631	1.642		2.409					6.993

[a] Restricted structures. Distances in angstroms, bond angles in degrees. [b] Frozen core calculations. [c] While α refers to the angles pertaining to the O—H···O H-bond, β corresponds to the C—H···O H-bonding angles.

Table 2 contains the corrected ab initio energies for the same aggregates. We should emphasize that combining the BSSE and vibrational corrections results in overcorrection of the calculations.[28,29] This problem arises because the frequencies are calculated on the uncorrected (for BSSE) surface, which has a deeper well. Thus, the intermolecular harmonic force constants are too large. For this reason, we state the interaction energies with the individual as well as the total corrections. Dimer I, the cyclic carboxylic acid structure that is experimentally observed in the gas phase and in solution, is included for comparison. As

(28) Bouteillier, Y.; Behrouz, H. *J. Chem. Phys.* **1992**, *96*, 6033.
(29) Turi, L.; Dannenberg, J. J. *J. Phys. Chem.* **1993**, *57*, 7899.

we noted in our earlier paper, the C—H···O bond formed in the dimeric structure **II** is insufficient to explain the aggregation in this first direction.[6] This can be seen from the fact that the interaction energy of dimer **II** is generally less than half that of dimer **I**. However, upon increasing the extent of aggregation, the cooperativity eventually increases the interaction energies to more than half the value for dimer **I**. Thus, the linear H-bonding cooperativity is sufficient to reverse this tendency with respect to ΔH.

The geometries of the aggregates are presented in Table 3. Several trends are immediately evident. The intermolecular O···O and O···H distances across the H-bonds decrease with increasing aggregate size. On the other hand, the corresponding O···C and O···H distances for the C—H···O H-bond increase. These observations suggest that the O—H···O interactions become stronger with increasing aggregation but the C—H···O interactions become weaker. Thus, the total cooperative effect is the sum of two divergent components. These data clearly show trends for the C—O bond to shorten and the C═O bond to lengthen as the aggregate grows. While not all MO methods are converging toward the experimental (crystal) molecular geometries because they underestimate the C—O and/or overestimate the C═O bond lengths, this trend is appropriate as the two bond lengths do shorten and lengthen, respectively, upon changing from the gas phase[30] to the crystal. The translation vector, **d** (the distance between repeating points in two adjacent units of two molecules), is not converging toward the experimental value (going from 7.003 to 7.035 Å for HF/6-31G). Thus, while the molecular geometry and H-bonding distances are improving with unidirectional aggregation, the crystal unit cell is not. Consideration of the aggregation in the other two directions is necessary.

The geometrical data shed light on the small extent of cooperativity in this direction predicted by the semiempirical methods. We have previously noted that these methods (especially AM1) tend to underestimate O—H···O interactions; however, AM1 is quite good at estimating the C—H···O interactions.[29] We suggest that the artifactually low cooperativity expected for the O—H···O interaction is roughly canceled by the decrease in the C—H···O interaction at the AM1 level.

Aggregation in the Second Direction: Stacking. The second direction that we consider involves stacking the "chains". We calculated various "stacks" containing different numbers of chains and chain lengths. We shall use the notation $N \times M$, where N is the number of chains in the stack and M is the number of molecules per chain. Tables 4–6 present the energetic and geometrical data. Only AM1 and PM3 among the semiempirical methods are capable of treating the stacking phenomenon. SAM1 is unable to find suitable stacking potential minima. The data of Table 4 indicate that adding N molecules to an $N \times M$ aggregate to form an $N \times (M + 1)$ stack, which would create N new interactions in the first direction, stabilizes the aggregate by increasingly more than N times the interaction energy (for $N = 1$) as N grows. Thus, increasing the size of the stack (in the second direction) cooperatively enhances the interaction energy for increasing the chain (in the first direction). This provides support for the concept of interdimensional cooperativity. One should note that AM1, which did not predict cooperativity in the first dimension when individual chains were considered (see above), clearly does predict cooperativity in this same direction when the chains are stacked.

The interactions between chains in a stack are the weakest of the three distinct directional interactions (see Table 5). The chains appear to be held together by a what may be a very weak C—H···O interaction between a second methyl C—H bond and an OH oxygen in an adjacent chain (see Figure 2). The C—H···O orientation is not ideal, as the methyl group conformation optimizes the stronger C—H···O interactions of the other two C—H bonds (one in the chain, the other is used in the third direction). In fact, the shortest H···O distance is about 3.6 Å, which is rather long for a H-bond. Table 5 gives the interaction energies for the incremental addition of chains of varying length to the growing aggregate. These interactions are mildly attractive at best (as they are repulsive with SAM1, the structures could not be optimized). After CP correction, the ab initio values descend to the order of those calculated by AM1. One is even slightly repulsive. ZPVE correction would further reduce the interaction, but this would lead to overcorrection (as noted above). The interaction of a stack of N chains with another chain depends upon the value of N. Thus, adding a $1 \times M$ chain to a $2 \times M$

(30) (a) van Eijck, B. P.; van Opheusden, J.; van Schaik, M. M. M.; van Zoeren, E. *J. Mol. Spectrosc.* **1981**, *86*, 465. (b) Caminati, W.; Scappani, F.; Corbelli, G. *J. Mol. Spectrosc.* **1979**, *75*, 327. (c) Derissen, J. L. *J. Mol. Struct.* **1971**, *7*, 67.

Table 4. Hydrogen-Bonding Energies[a] (kcal/mol) for Adding N Acetic Molecules to $N \times M$ Stacks To Form $N \times (M + 1)$ Aggregates (See Explanation in Text)

	M				
N	1	2	3	4	5
			AM1		
1	−4.79	−4.73	−4.79	−4.77	−4.79
2		−9.66	−9.68	−9.71	−9.72
3		−14.56	−14.65		
4		−19.49	−19.55		
			PM3		
1	−4.87	−5.40	−5.51	−5.54	−5.57
2		−11.03	−11.22	−11.31	−11.42
3		−16.60	−16.97		
4		−22.24	−22.58		
			HF/6-31G[b]		
1	−11.28	−11.70	−11.99	−12.11	−12.17
	(−9.44)	(−9.85)	(−10.12)	(−10.23)	(−10.29)
2		−24.53			
		(−19.44)			
3		−38.12			
		(−29.71)			
			HF/6-31G(d)		
1	−8.75	−9.02	−9.18		
	(−7.09)	(−7.34)	(−7.49)		
2		−18.92			
		(−14.21)			

[a] Enthalpies for AM1 and PM3. [b] Ab initio values in parentheses correspond to CP corrected interaction energies.

Table 5. Incremental Interaction Energies[a] (kcal/mol) between Chains of Different Size in Two-Dimensional Stacked $N \times M$ Aggregates

	M				
N	2	3	4	5	6
			AM1		
2	−0.60	−0.80	−0.90	−1.07	−1.20
3	−0.40	−0.57	−0.74		
4	−0.51	−0.71	−0.82		
			PM3		
2	−0.89	−1.12	−1.32	−1.55	−1.83
3	−0.57	−0.74	−0.98		
4	−0.76	−1.00	−1.10		
			HF/6-31G		
2	−4.15	−5.29			
	(−1.59)	(−1.44)			
3	−2.04	−3.94			
	(+0.06)	(−0.28)			
			HF/6-31G(d)		
2	−3.18	−4.32			
	(−0.80)	(−0.54)			
			HF/6-31G(d,p)		
2	−3.19				
	(−0.77)				

[a] Ab initio values in parentheses correspond to CP corrected interaction energies.

Table 6. Selected H-Bonding Geometries and Unit Cell Dimensions at Different Levels of Theory[a]

$N \times M$	C=O	C—O	O···O	O···HO	O···C	O···HC	b	c	α	d
					AM1					
2 × 2	1.237	1.360	3.061	2.097	3.341	2.246	5.390	5.390		
3 × 2	1.238	1.360	3.057	2.096	3.342	2.243	5.393	5.398	86.70	
4 × 2	1.238	1.360	3.054	2.095	3.345	2.245	5.420	5.421	86.52	
2 × 3	1.238	1.359	3.055	2.090	3.346	2.256	5.436	5.437	84.79	7.332
			3.055	2.090	3.346	2.257				
3 × 3	1.238	1.359	3.049	2.088	3.348	2.252	5.471	5.480	85.11	7.406
			3.052	2.089	3.353	2.258				
4 × 3	1.239	1.359	3.049	2.088	3.352	2.254	5.493	5.493	84.98	7.420
			3.049	2.088	3.352	2.254				
2 × 4	1.239	1.358	3.051	2.087	3.352	2.255	5.484	5.486	84.32	7.364
			3.052	2.087	3.352	2.256				
3 × 4	1.239	1.358	3.047	2.086	3.353	2.252	5.514	5.516	84.34	7.405
			3.050	2.087	3.355	2.258				
4 × 4	1.239	1.358	3.047	2.086	3.356	2.256	5.523	5.524	84.43	7.422
			3.047	2.086	3.356	2.256				
2 × 5	1.239	1.357	3.050	2.086	3.352	2.257	5.498	5.510	84.02	7.367
			3.051	2.086	3.354	2.259				
2 × 6	1.239	1.357	3.049	2.084	3.354	2.257	5.526	5.533	83.58	7.370
			3.049	2.084	3.355	2.258				
					PM3					
2 × 2	1.223	1.347	2.723	1.792	3.516	2.495	5.190	5.193		
3 × 2	1.223	1.348	2.721	1.794	3.512	2.487	5.115	5.286	86.41	
4 × 2	1.223	1.348	2.719	1.793	3.502	2.480	5.129	5.303	86.09	
			2.721	1.794	3.514	2.495				
2 × 3	1.225	1.344	2.721	1.785	3.514	2.518	5.342	5.345	82.40	7.039
			2.722	1.786	3.521	2.525				
3 × 3	1.225	1.345	2.716	1.785	3.524	2.500	5.145	5.277	86.10	7.115
			2.719	1.786	3.528	2.506				
4 × 3	1.225	1.345	2.720	1.786	3.506	2.518	5.351	5.356	82.22	7.040
			2.720	1.786	3.507	2.519				
2 × 4	1.226	1.343	2.716	1.781	3.535	2.515	5.184	5.222	86.11	7.105
			2.716	1.781	3.536	2.516				
3 × 4	1.226	1.343	2.714	1.781	3.533	2.510	5.164	5.272	86.05	7.121
			2.714	1.783	3.533	2.511				
4 × 4	1.226	1.343	2.715	1.782	3.530	2.507	5.175	5.279	85.93	7.125
			2.715	1.782	3.532	2.510				
2 × 5	1.226	1.342	2.716	1.779	3.534	2.520	5.237	5.281	84.79	7.092
			2.716	1.779	3.538	2.524				
2 × 6	1.227	1.341	2.714	1.777	3.542	2.521	5.192	5.228	86.13	7.115
			2.714	1.778	3.542	2.521				
					HF/6-31G					
2 × 2	1.220	1.342	2.755	1.795	3.409	2.380	4.818	4.818		
3 × 2	1.220	1.343	2.763	1.804	3.386	2.343	4.892	4.892	86.44	
2 × 3	1.223	1.337	2.738	1.775	3.484	2.456	4.909	4.910	87.71	7.080
3 × 3	1.223	1.338	2.738	1.776	3.454	2.418	4.905	4.911	86.68	7.139
					HF/6-31G(d)					
2 × 2	1.195	1.322	2.858	1.911	3.476	2.439	4.918	4.920		
2 × 3	1.197	1.319	2.840	1.894	3.539	2.506	5.016	5.017	88.29	7.080
					HF/6-31G(d,p)					
2 × 2	1.195	1.321	2.852	1.909	3.458	2.419	4.914	4.915		
exptl[2]	1.206	1.321	2.631	1.642		2.409	3.963	5.762	90.00	6.993

[a] Distances in angstroms, bond angles in degrees.

stack provides less stabilization than combining two $1 \times M$ chains or adding a $1 \times M$ chain to a $3 \times M$ stack. The analysis of the pairwise and nonadditive contributions below will show that the interaction in the second direction is cooperative.

As can be seen from Table 6, the molecular geometries and H-bonding distances continue to reasonably converge, but the unit cell dimensions, particularly **b**, do not. While AM1 is primarily in error for the unit cell dimension, **b**, and the translation vector, **d**, PM3 and the HF calculations are primarily in error for the cell dimensions ***b*** and ***c*** (see Figure 4). Thus, the two-dimensional model remains inadequate to fully explain the crystalline intermolecular interactions for acetic acid.

Aggregation in the Third Direction: Microcrystals. The individual stacks interact essentially through C—H···O H-bonds (involving the third methyl C—H bond), as can be seen from careful inspection of Figure 3. Each stack is roughly perpendicular to its neighbors. Each molecule has two C—H···O interactions (one each as donor and receptor) with two different molecules in different chains of an adjacent stack. Each successive molecule in a chain interacts with a stack on the opposite side of the chain. The interaction energies are presented in Table 7. We define the size of the microcrystals as $L \times M \times N$, where L is the number of stacks and M and N retain their former definitions. The size of the aggregates precluded use of ab initio calculations for these structures. The microcrystals are minima on all the semiempirical potential surfaces, so AM1, PM3, and SAM1 results are presented.

Table 7. Incremental Stabilization Energies (kcal/mol) between Stacked 3 × 3 Aggregates in $L \times 3 \times 3$ Aggregates

	L		
method	2	3	4
SAM1	+5.46		
PM3	−7.21		
AM1	−7.26	−7.55	−7.67

Table 8. Selected H-Bonding Distances and Unit Cell Parameters (Å) in Three-Dimensional Orthorhombic $L \times 3 \times 3$ (L = 2, 3, 4) Aggregates[a]

L	C=O	C—O	O···O	O···HO	O···C	O···HC	a	b	c	d
					SAM1					
1	1.257	1.377	2.735	1.778	3.045	1.950		5.032	5.035	7.118
			2.738	1.781	3.047	1.953				
2	1.257	1.377	2.736	1.778	3.069	1.977		4.992	5.103	7.139
			2.742	1.790	3.071	1.976				
					PM3					
1	1.225	1.345	2.714	1.788	3.535	2.506		5.027	5.120	7.175
			2.717	1.789	3.540	2.514				
2	1.225	1.345	2.710	1.786	3.548	2.520		5.084	5.088	7.193
			2.712	1.787	3.552	2.526				
					AM1					
1	1.239	1.359	3.050	2.092	3.353	2.250		5.261	5.291	7.461
			3.052	2.093	3.356	2.254				
2	1.239	1.359	3.032	2.081	3.365	2.269		5.059	5.487	7.463
			3.037	2.084	3.370	2.274				
3	1.239	1.359	3.027	2.080	3.372	2.276	13.043	5.042	5.549	7.498
			3.032	2.084	3.376	2.281				
4	1.239	1.359	3.025	2.078	3.373	2.277	13.042	5.033	5.555	7.496
			3.028	2.079	3.377	2.283				
exptl	1.206	1.321	2.631	1.642		2.409	13.225	3.963	5.762	6.993

[a] For comparison we included the 3 × 3 orthorhombic aggregates (as 1 × 3 × 3) in the table.

Table 9. Pairwise Interactions (kcal/mol) between Stacked Chains in the 1 × 4 × 4 Aggregate and between Interacting Stacks in the 4 × 3 × 3 Aggregate

	pairwise interaction						
aggregate	1–2	1–3	1–4	2–3	sum of pairwise interactions	calculated interaction energy	nonadditivity
1 × 4 × 4	−0.86	+0.25	+0.14	−0.80	−1.88	−2.47	−0.59
4 × 3 × 3	−7.42	+0.88	+0.75	−7.42	−19.75	−22.92	−3.17

[a] No correction for distortion.

Due to the significantly larger size of AMPAC 4.5 compared to AMPAC 2.1, we could not calculate microcrystals larger than 2 × 3 × 3 (18 molecules) for SAM1 and PM3. The microcrystals are minima on the SAM1 surface, despite the observation that the stacking interaction is repulsive (see above) at this level of calculation. Only AM1 and PM3 predict attractive interactions in all three directions.

The geometrical data of Table 8 indicate that, when all three directions of aggregation are considered, the unit cell dimensions (as well as the molecular dimensions) converge to their experimental values as the size of the aggregate increases. The agreement between the experimental and AM1 unit cell parameters is striking, with the exception of **b**, which is due to the familiar failing of AM1 to accurately predict the H-bonding distances in O—H···O interactions. Nevertheless, even in this unit cell direction, the growing microcrystal is converging in the right direction. One should recall (Table 6) that the HF calculations do not accurately predict the experimental value of **b** in the stacks (although they are somewhat better than AM1).

Cooperativity. Cooperativity can be arbitrarily divided into two effects: (a) the pairwise interactions between individual units and (b) the remaining "nonadditive" contribution.[31] Table 9 illustrates the pairwise and nonadditive contributions to the interactions in the second and third directions in a 4 × 4 stack and a 4 × 3 × 3 microcrystal. Within the 4 × 4 stack there are three attractive (1–2, 2–3, and 3–4) and three repulsive (1–3, 2–4, and 1–4) interactions. By symmetry, the 1–2 and 3–4 and the 1–3 and 2–4 interactions are equivalent. Adding the pairwise interactions predicts a stabilization of 2.20 kcal/mol, 0.27 kcal/mol lower than that predicted by the calculation on the supermolecule, after correction for the additional distortions in the sum of the pairwise interactions. We have encountered this phenomenon in other studies of molecular aggregation.[32] It is discussed in detail elsewhere.[27] The apparent reason for the repulsion between the nth and $(n+2)$th chains lies in the structure of the chain which alternates the orientations of the methyl groups in adjacent chains (see Figure 2). The 1–4 repulsion is due to the distortions of the individual chains (or stacks) upon aggregation to form a stack (or microcrystal). At long distances, the attraction between the components of each pair tend toward zero, leaving only the distortion energies. This phenomenon is discussed in detail elsewhere.[27]

This analysis helps explain the difference in the incremental stacking interactions (Table 5). Thus adding a $1 \times M$ chain to a $1 \times M$ chain creates one (stabilizing) 1–2 interchain interaction. Adding another $1 \times M$ chain to the $2 \times M$ chain creates a second pairwise 1–2 interaction (stabilizing), a pairwise 1–3 interaction (destabilizing), and a nonadditive component. Adding a fourth $1 \times M$ to the $3 \times M$ chain creates another 1–2, 1–3, and 1–4 interaction plus a modification in the nonadditive component. The stacking interaction for $1 \times M$ plus $2 \times M$ is less than that for $1 \times M$ plus $1 \times M$ because of the repulsive 1–3 interaction in the former. The greater stabilization shown for $1 \times M$ plus $3 \times M$ than for $1 \times M$ plus $2 \times M$ indicates cooperativity in the second direction because the new interactions contain both (1–2 and 1–3) those expected for the formation of the $3 \times M$ plus a slightly repulsive 1–4 interaction.

In the third direction, one can make a similar analysis. Table 9 presents the pairwise and nonadditive interactions for a 4 × 3 × 3 microcrystal. Once again, the interactions between adjacent units are stabilizing, while those between nonadjacent units are repulsive. The major difference is that the stabilizations between adjacent units is much greater (due to the better orientation of the C—H···O interactions, see Figure 3) than that in the second direction. Although the nonadditive effect in the third direction of the 4 × 3 × 3 microcrystal is much greater than that for the second direction of the 4 × 4 stack (1.53 vs 0.27 kcal/mol), it is a smaller fraction of the total interaction.

(31) For example, see: Hankins, D.; Moskowitz, J. W.; Stillinger, F. H. *J. Chem. Phys.* **1970**, *53*, 4544.
(32) Turi, L.; Dannenberg, J. J. *Chem. Mater.* **1994**, *6*, 1313.
(33) Turi, L.; Dannenberg, J. J., to be published.

The analysis presented above clearly indicates the dangers inherent in any attempt to explain the intermolecular interactions with a theory dependent strictly upon pairwise potential functions. Pairwise functions would have to be different for different sized aggregates and (presumably) for different orientations of the monomeric units in the aggregate.

The Process of Self-Assembly. The acetic acid crystal provides insight into the mechanism of molecular recognition in crystal formation. The strongest intermolecular interactions are those of the pairs of H-bonds (one O—H···O and one C—H···O) that form the chains. However, bimolecular interactions involving two O—H···O H-bonds (as in **I**) are more stabilizing. Thus, if the crystal were to grow from an original dimer, **I**, it might break one of the O—H···O bonds and add a third molecule. Enthalpically, this is not too unfavorable as the resulting trimer has two of each (O—H···O and C—H···O) interaction, while the equivalent dimer **I** and a monomer have only the H-bonds in **I**. If one considers the formation of a tetramer from two dimers **I**, the situation is less favorable, as there are four O—H···O interactions in the two dimers vs only three (plus three C—H···O) in the tetramer. Continuing this reasoning, one can see that any even quantity of monomers will lose one O—H···O interaction but gain $n - 1$ C—H···O interactions (where n is the number of monomers) upon transformation from $n/2$ dimers **I** to a single oligomeric chain. Ultimately, the single chain must become enthalpically favorable since (a) the $n - 1$ C—H···O interactions will more than compensate for the single lost O—H···O interaction as the chain grows and (b) the O—H···O interactions increase in strength as the chain grows due to the cooperativity. In solution, the entropic component of ΔG dominates, so the dimeric structure prevails. In a crystal, however, the intermolecular degrees of freedom are all essentially lost, so the entropic differences become much less important, allowing the enthalpic component to dominate.

The two ends of a growing chain are different. One end has an uncomplexed carboxyl group, the other the carbonyl of the carboxyl and a methyl group (see Figure 1). Thus, the first (carboxyl) end can bind another monomer either to continue the chain or to form a local (2) O—H···O H-bond interaction similar to that of **I**. The other (methyl) end can only accommodate a monomer in the chainlike manner. Thus, growth rates of the chains should be different at each end. Another mechanism for the original nucleation might be maintaining the initial dimer, **I**, while growing the chain in two equivalent directions (each chain end would have methyl and a C=O available for attaching another monomer). Eventually, the H-bonds in the original dimer could break, creating two growing chains, or the original dimer could remain as a flaw in the crystal.

Growths in the second and third directions are more difficult to imagine. The rather weak interactions between the chains in the second direction suggest that the greater stabilizing interactions in the third direction might initially be more important. However, it is difficult to visualize a mechanism for the interactions between the stacks unless stacks already exist. Probably, growth in the second and third directions are coupled. Initially, these processes probably have a relatively unfavorable balance between ΔH and ΔS, as many degrees of freedom are lost in the aggregation process, but the resulting enthalpic stabilization/molecule is small (compared to chain growth). Thus, forming the initial microcrystal from the chains is probably the slow step in the nucleation process.

Conclusions

The methods used in this study, ab initio and semiempirical molecular orbital calculations, are clearly capable of predicting the crystal structure of acetic acid, despite its somewhat unusual nature. Furthermore, the results of the calculations allow us to evaluate and understand the contributions of the various factors to the establishment of that structure. Thus, these methods ought to be useful for studying other molecular recognition and self-assembly phenomena as well as additional crystal structures. The importance of the cooperative effects, particularly the "nonadditive" part, shows that pairwise potentials are not likely to be generally applicable in different phases, where the extent of aggregations will significantly differ. Thus, in the gas phase, acetic acid will be monomeric or dimeric, in the liquid primarily dimeric, but entirely different in the solid phase.

Acknowledgment. This work was supported in part by grants from the BHE-PSC, NSF, and IBM Corporation.